

4 Modification of Carbene Ligands: Aminolysis

4.1 Background

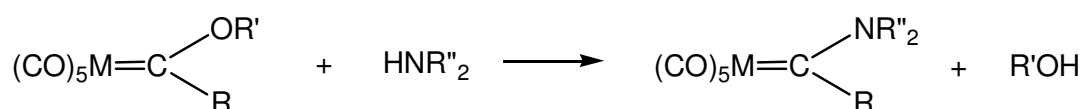
4.1.1 Overview

Aminocarbene complexes of transition metals are being increasingly seen as versatile starting materials for the synthesis of nitrogen-containing heterocycles^[1-10]. Their behaviour has been found to be fundamentally different from that of related alkoxy carbene complexes since nitrogen ylides, derived from ketene intermediates, have been isolated and shown to rearrange upon thermolysis to give pyrrolinones by 1,2 and 1,4 nitrogen to carbon migrations of alkyl groups.

4.1.2 Synthesis of aminocarbene complexes

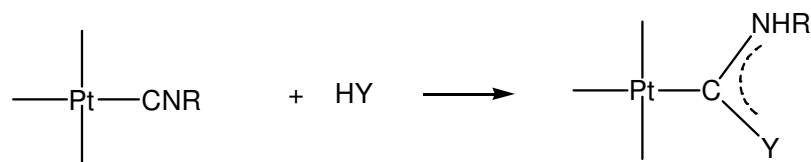
Due to the electrophilic nature of the carbene carbon of Fischer carbene complexes, nucleophilic attack on the carbene carbon is possible. Connor and Fischer first investigated the nucleophilic substitution reactions of Fischer carbene complexes with amines^[11], after the synthesis of the first aminocarbene complexes by Klabunde^[12]. It was found that the nucleophilic attack of the nitrogen lone pair on the carbene carbon atom leads to the elimination of alcohol and the formation of the aminocarbene product. This

outcome was rationalised by the view that the $M(CO)_5$ -moiety is electronically similar to a carbonyl oxygen atom, so that the reaction is similar to the aminolysis of esters to form amides.



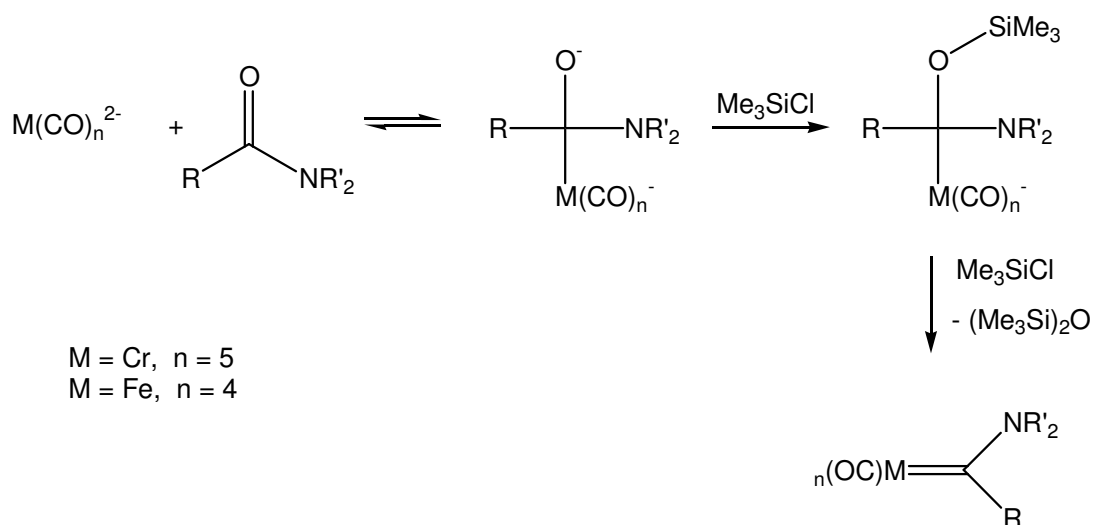
Scheme 4.1 Aminolysis of Fischer carbene complexes

As with the synthesis of alkoxy-carbene complexes, alternative synthetic methods were developed. Platinum complexes containing an isocyanide ligand easily undergo attack by protic nucleophiles such as amines or alcohols to yield metal-carbene derivatives (Scheme 4.2) through attack at the terminal carbon atom ^[13;14].



Scheme 4.2 Nucleophilic attack on isocyanide ligand of platinum complexes

Another example is the very efficient method for the preparation of chromium aminocarbene complexes introduced by Hegedus^[15] (Scheme 4.3). It involves the reaction of $Cr(CO)_5^{2-}$ with tertiary amides in the presence of chlorotrimethylsilane. The reaction proceeds via nucleophilic addition of $Cr(CO)_5^{2-}$ to the carbonyl group of an amide followed by the O-silylation of the adduct. Addition of excess chlorotrimethylsilane then affords the elimination of hexamethyldisiloxane and the formation of product aminocarbene ensues.



Scheme 4.3 Hedgedus synthesis of aminocarbene complexes

Since the synthesis of the first aminocarbene complexes, it was recognized that these complexes are more stable than their alkoxy analogues. This was ascribed to greater participation of the nitrogen lone pair compared to oxygen in stabilizing the electrophilic carbene carbon atom. The observations of Kreissl that $[\text{W}(\equiv\text{CC}_6\text{H}_4\text{Me-4})\text{Cp}(\text{CO})_2]$ reacts with hydrogen chloride to form the acyl complex $[\text{W}(\eta^2\text{-C}(\text{O})\text{CH}_2\text{C}_6\text{H}_4\text{Me-4})\text{Cp}(\text{CO})\text{Cl}_2]$ ^[16], but the same reagent with $[\text{W}(\equiv\text{CNEt}_2)\text{Cp}(\text{CO})_2]$ affords the aminomethylene complex $[\text{W}(=\text{CHNEt}_2)\text{CpCl}(\text{CO})_2]$ ^[17] confirmed the indications that amino substituents could stabilize carbene ligands bound to mid-valent Group VI metal centres.

4.1.3 Binuclear aminocarbene complexes

After Fischer's first paper^[18] reporting the synthesis of several binuclear alkoxy-carbenes of the type $[\text{M}_2(\text{CO})_9\{\text{C}(\text{OR}')\text{R}\}]$ ($\text{M} = \text{Mn}, \text{Tc}, \text{Re}$; $\text{R} = \text{alkyl or aryl}$; $\text{R}' = \text{alkyl}$)^[19], there was some uncertainty as to whether the carbene ligand was in the equatorial or the axial position (C_s or C_{4v} symmetry) relative to the Mn-Mn bond when the carbene was bulky. X-ray crystal structure determination of $[\text{Mn}_2(\text{CO})_9\{\text{C}(\text{OCH}_3)\text{C}_6\text{H}_5\}]$ proved the carbene occupies the equatorial position^[20].

Post and Watters were the first to report the preparation and characterization of methylaminocarbene of binuclear metal carbonyl complexes^[21]. From the infrared and Raman data they obtained, they concluded that both complexes $[\text{Mn}_2(\text{CO})_9\{\text{C}(\text{NHCH}_3)\text{CH}_3\}]$ and $[\text{Re}_2(\text{CO})_9\{\text{C}(\text{NHCH}_3)\text{CH}_3\}]$ were equatorially substituted. While the dirhenium aminocarbene could be isomerized into a *cis-trans* mixture about the C-N bond, no *trans* dimanganese aminocarbene complex could be isolated.

4.1.4 Focus of this study

In order to investigate the possibility of manipulating the orientation of carbene ligands of the dimanganese carbene complexes synthesized in Chapter 2, the aminolysis of these compounds were carried out.

After successful aminolysis with ammonia gas, the reactions were repeated with the more bulky secondary amines, diethylamine and diisopropylamine. These attempts did not prove possible, and could be explained by the observation made by Werner^[22]. The mechanism proposed by Werner for aminolysis involves more than one amine to activate the carbene carbon atom. This implies that only small amines will affect this type of reaction in already hindered carbene complexes. The reaction of the primary amine, propylamine, more bulky than ammonia but small enough to be accommodated as substituent on the carbene ligand of the binuclear complexes, was then attempted and proved successful.

Once again, the rhenium analogues of the dimanganese monocarbene complexes were also synthesized and characterized for comparison of the steric and electronic properties of the amino-substituted carbene ligands. Figure 4.1 illustrates the complexes synthesized in this chapter.

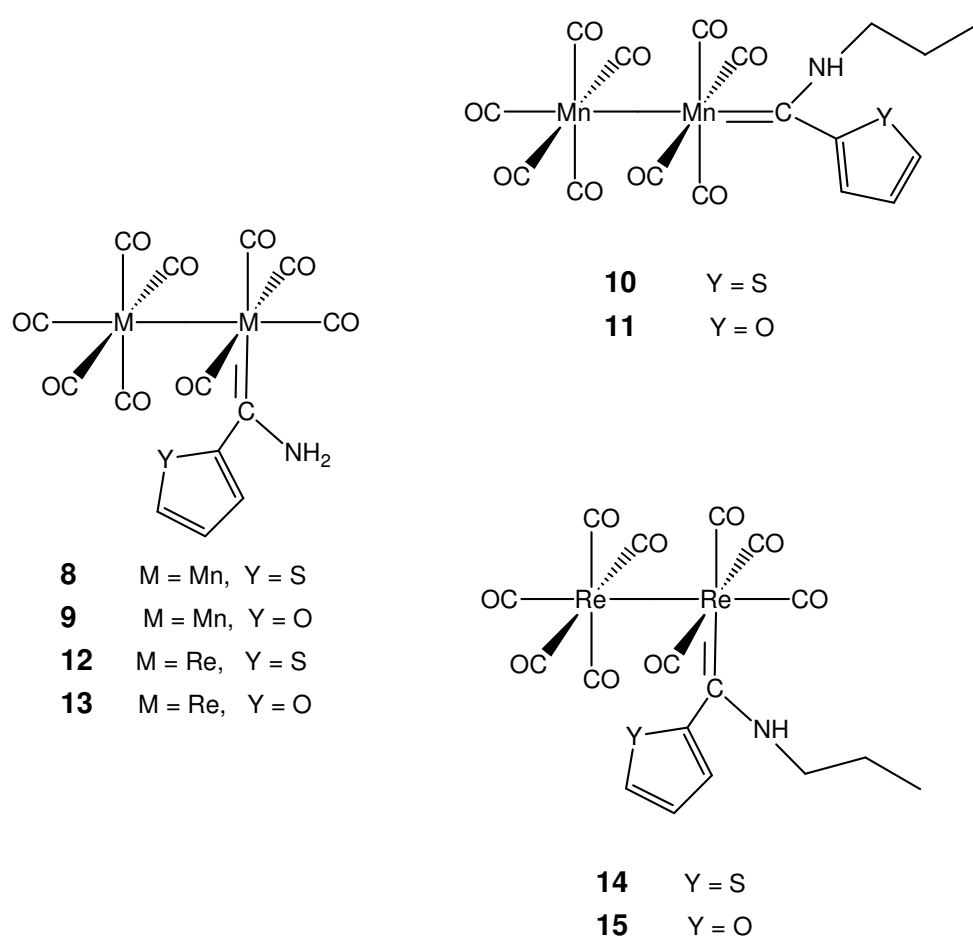
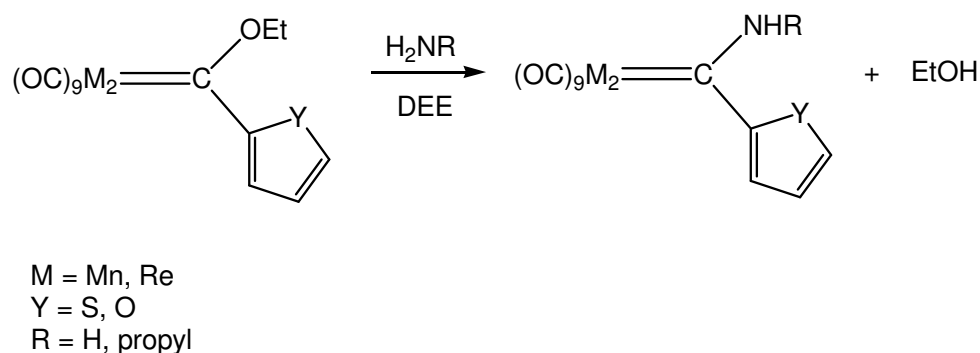


Figure 4.1 Binuclear aminocarbene complexes synthesized

4.2 Synthesis

Synthesis of the aminocarbene complexes was carried out as described by Klabunde and Fischer^[12]. A slow stream of ammonia was bubbled through a solution of the binuclear ethoxycarbene complexes dissolved in diethyl ether at room temperature. The colour of the solution changed rapidly from red to orange. After thin layer chromatography confirmed that all the ethoxycarbene complex had been converted, the solvent was removed and the aminocarbene complexes were purified by column chromatography on aluminium oxide, and complexes **8**, **9**, **12** and **13** were obtained in yields greater than 85%.



Scheme 4.4 Aminolysis of binuclear ethoxycarbene complexes

The procedure was repeated, but instead of bubbling ammonia gas through the solution, excess propylamine was added to the reaction mixture in ether, to obtain the propylamine-substituted carbene complexes **10**, **11**, **14** and **15** in yields ranging from 75 to 87%.

4.3 Characterisation

The aminocarbene complexes **8** - **15** were characterized spectroscopically in solution and in the solid state by mass spectrometry and X-ray crystallography.

4.3.1 NMR Spectroscopy

In the 1H NMR spectra of the manganese complexes **8** - **11**, the heteroarene and amine protons are duplicated in a major and minor isomer. The same duplication of carbon resonances was observed in the ^{13}C NMR spectra for these four complexes. We suspect that in solution, a mixture of the equatorial

and axial isomers exists. However, it is unclear which set of signals belongs to which isomer.

Both the ^1H and ^{13}C NMR spectra of complex **8** and **9** were recorded in acetone- d_6 , as no clearly resolved spectra could be obtained in CDCl_3 . The rest of the complexes were analysed in the deuterated chloroform, and better resolution was achieved than for **8** and **9**. The same numbering system of the carbon atoms and protons of the heteroarene substituents was used as before.

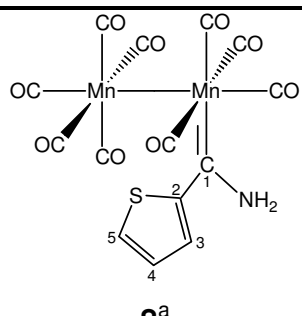
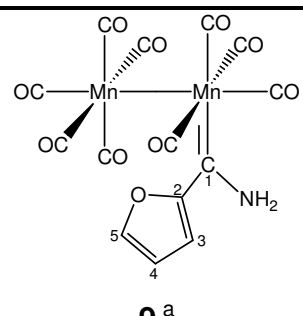
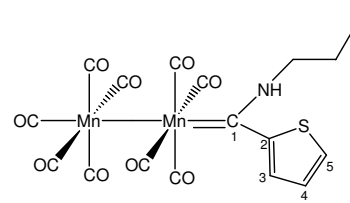
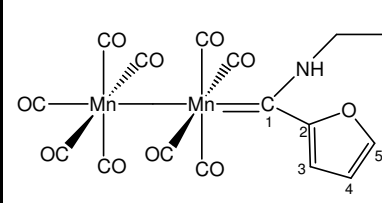
4.3.1.1 ^1H NMR Spectroscopy

The ^1H NMR data of **8** - **15** are summarized in Table 4.1. For **8** and **9**, the major and minor isomers (duplication of signals) were easily distinguishable, but the signals in the spectrum of **10** and **11** respectively were too broadened, so that no J couplings, nor the duplication of the proton resonances of the isomers were observed.

Figure 4.2 is an expansion of the aromatic region in the ^1H NMR spectrum recorded for **8**, showing the duplication of the thienyl ring protons, the major and minor isomer having different signal intensities. The N-H proton signals overlap, so that assignment of the N-H protons of both isomers cannot be done.

The broadening of signals in the spectra of **8** - **11** might be due to the paramagnetic nature of $\text{Mn}(0)$, possibly present as a decomposition product. No consistent upfield or downfield shift of the chemical shift values of the ring protons could be observed.

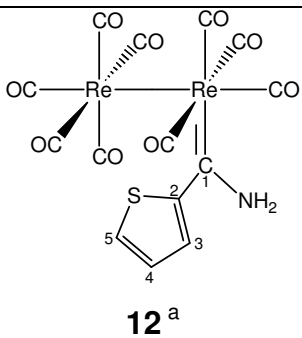
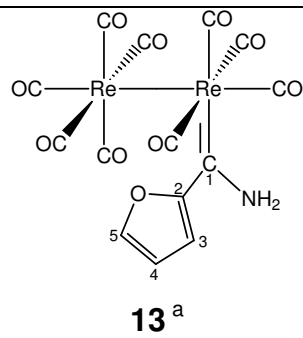
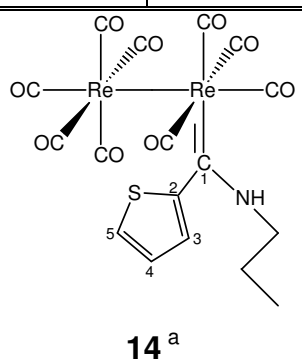
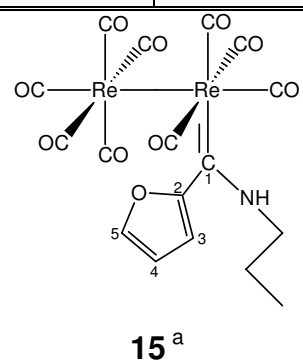
Table 4.1 ^1H NMR data of complexes **8** - **15**

Assignment	Complexes			
	Chemical shifts (δ , ppm) and coupling constants (J , Hz)			
	 8^a		 9^a	
Proton	<i>Isomer a</i>	<i>Isomer b</i>	<i>Isomer a</i>	<i>Isomer b</i>
H3	7.81 d (4.2)	7.95	7.50	6.79
H4	7.24 d (4.4)	7.31	6.78	n.o.
H5	7.59 d (2.1)	7.74	7.96	7.54
-NH ₂	10.57, 9.78	9.95, n.o. signal overlap	10.49, 9.90	9.48, n.o. signal overlap
Assignment	 10^b		 11^b	
Proton	<i>Peaks too broad to distinguish between isomers</i>			
H3	7.47		7.41	
H4	6.82		6.75	
H5	7.05		7.64	
-NCH ₂ CH ₂ CH ₃	1.67		1.74	
-NCH ₂ CH ₂ CH ₃	1.24		1.00	
-NCH ₂ CH ₂ CH ₃	0.96		0.84	
-NH	n.o.		n.o.	

 a) Spectra recorded in acetone- d_6

 b) Spectra recorded in CDCl_3

Table 4.1 contd. ^1H NMR data of complexes **8 - 15**

Assignment	Complexes			
	Chemical shifts (δ , ppm) and coupling constants (J , Hz)			
	 12^a		 13^a	
Proton	δ	J	δ	J
H3	7.60 (dd)	5.2, 0.9	7.53 (dd)	5.0, 1.6
H4	7.19 (dd)	5.0, 3.9	6.62 (dd)	5.0, 3.9
H5	7.58 (dd)	4.0, 1.0	7.62 (dd)	3.8, 1.8
-NH ₂	8.32, 8.14 (s, s)	-	8.87, 8.03 (s, s)	-
Assignment	 14^a		 15^a	
Proton	δ	J	δ	J
H3	7.64 (dd)	5.0, 1.0	7.65	n.o.
H4	6.90 (dd)	5.0, 3.7	6.89	n.o.
H5	7.07 (dd)	3.6, 1.1	7.65	n.o.
-NCH ₂ CH ₂ CH ₃	1.18 (t)	7.0	1.24	n.o.
-NCH ₂ CH ₂ CH ₃	1.66 (tt)	7.2, 7.5	1.08	n.o.
-NCH ₂ CH ₂ CH ₃	0.94 (t)	7.4	0.99	n.o.
-NH	8.52 (s)	-	8.60	n.o.

 a) Spectra recorded in CDCl₃

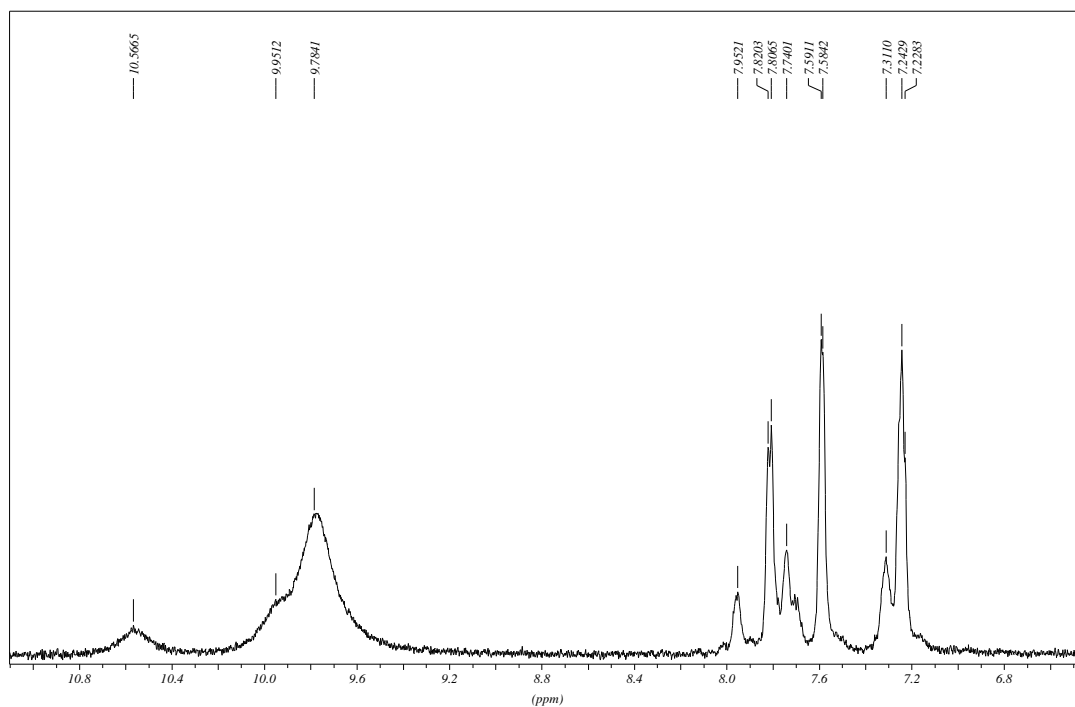


Figure 4.2 Expansion of the ^1H NMR spectrum of **8** in acetone- d_6 illustrating the presence of a major and minor isomer

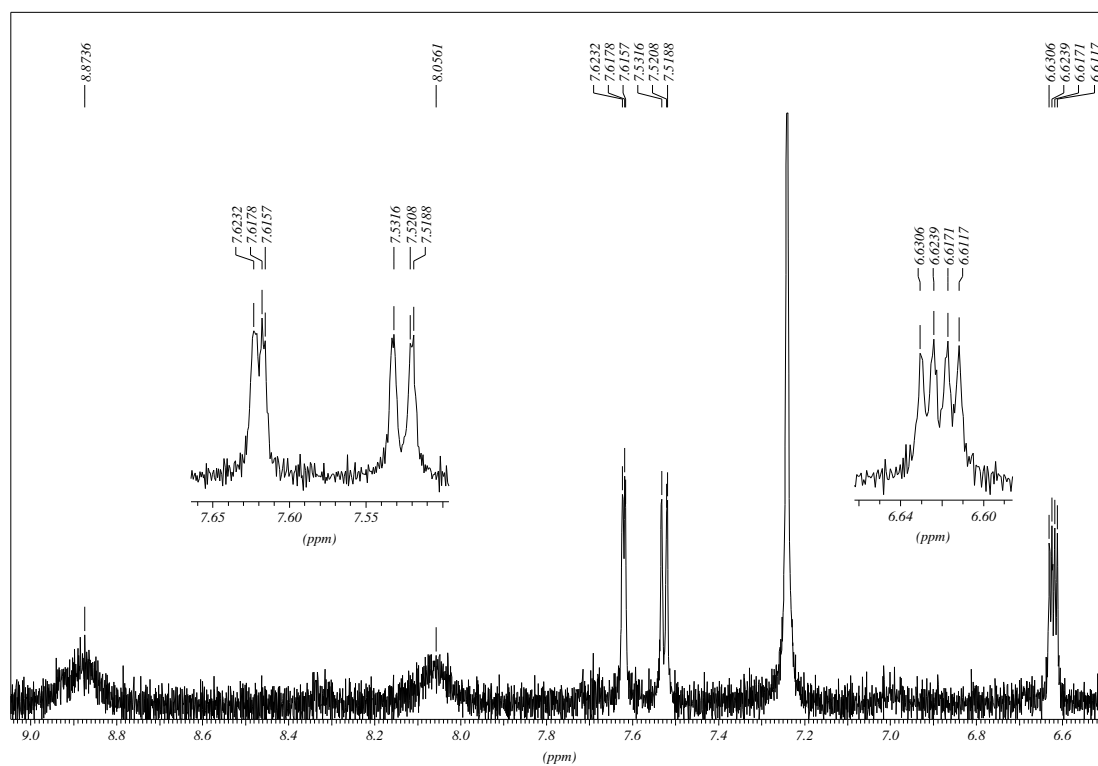


Figure 4.3 An expansion of the ^1H NMR spectrum of **13** in CDCl_3

4.3.1.1 ^{13}C NMR Spectroscopy

The ^{13}C NMR data of **8** - **15** are reported in Table 4.2 and 4.3. Better resolution of the signals was attained than for the ^1H NMR spectra, with the presence of a major and a minor isomer of the manganese complexes in solution clearly visible in the spectra. No ^{13}C NMR spectra could be obtained for **10** and **15** due to the decomposition of these complexes during spectrum recording.

Figure 4.4 shows the mixture of isomers present in solution for **11**, while the absence of a duplicated set of signals is apparent when looking at Figure 4.5, the ^{13}C NMR spectrum of the dirhenium aminocarbene **14**.

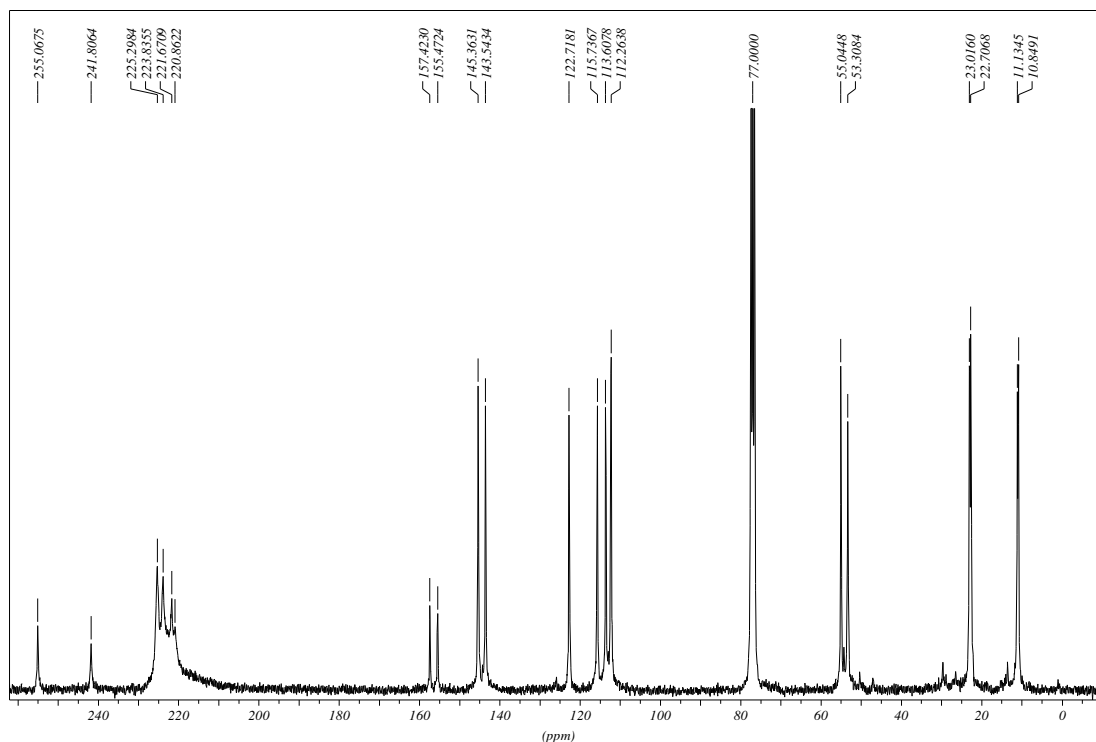


Figure 4.4 ^{13}C NMR spectrum of **11** in CDCl_3 , displaying duplication of carbon resonances for the two isomers

Table 4.2 ^{13}C NMR data of complexes **8**, **9**, **11** and **14**

Assignment	Complexes			
	8^a		9^a	
	<i>Isomer a</i>	<i>Isomer b</i>	<i>Isomer a</i>	<i>Isomer b</i>
Carbon	δ (ppm)	δ (ppm)	δ (ppm)	δ (ppm)
C1	269.6	262.6	275.4	267.6
C2	157.5	156.3	150.8	150.2
C3	133.8	135.9	121.0	117.3
C4	132.0	131.1	117.1	116.9
C5	132.1	131.1	123.5	120.9
M(CO) ₄	227.8	226.4	233.6	229.1
M(CO) ₅	225.7, 223.9	224.7, 222.8	228.4, 226.2	224.2, n.o. signal overlap
Assignment	11^b		14^b	
	<i>Isomer a</i>	<i>Isomer b</i>		
C1	255.1	241.8	239.3	
C2	157.4	155.5	150.4	
C3	122.7	115.7	127.0	
C4	113.6	112.3	124.2	
C5	145.4	143.5	128.2	
M(CO) ₄	225.3	223.8	199.9	
M(CO) ₅	221.7, n.o. signal overlap	220.9, n.o. signal overlap	193.9, 190.2	
-NCH ₂ CH ₂ CH ₃	55.0	53.3	56.5	
-NCH ₂ CH ₂ CH ₃	23.0	22.7	29.7	
-NCH ₂ CH ₂ CH ₃	11.1	10.8	10.9	

 a) Spectra recorded in acetone-d₆

 b) Spectra recorded in CDCl₃

Table 4.3 ^{13}C NMR data of complexes **12** and **13**

Assignment	Complexes ^a	
	12	13
Carbon	δ (ppm)	δ (ppm)
C1	268.8	238.0
C2	166.7	n.o.
C3	131.6	126.0
C4	128.9	114.3
C5	130.8	145.8
M(CO) ₄	198.8	200.5
M(CO) ₅	196.2, 184.0	197.9, 184.8

a) Spectra recorded in CDCl_3

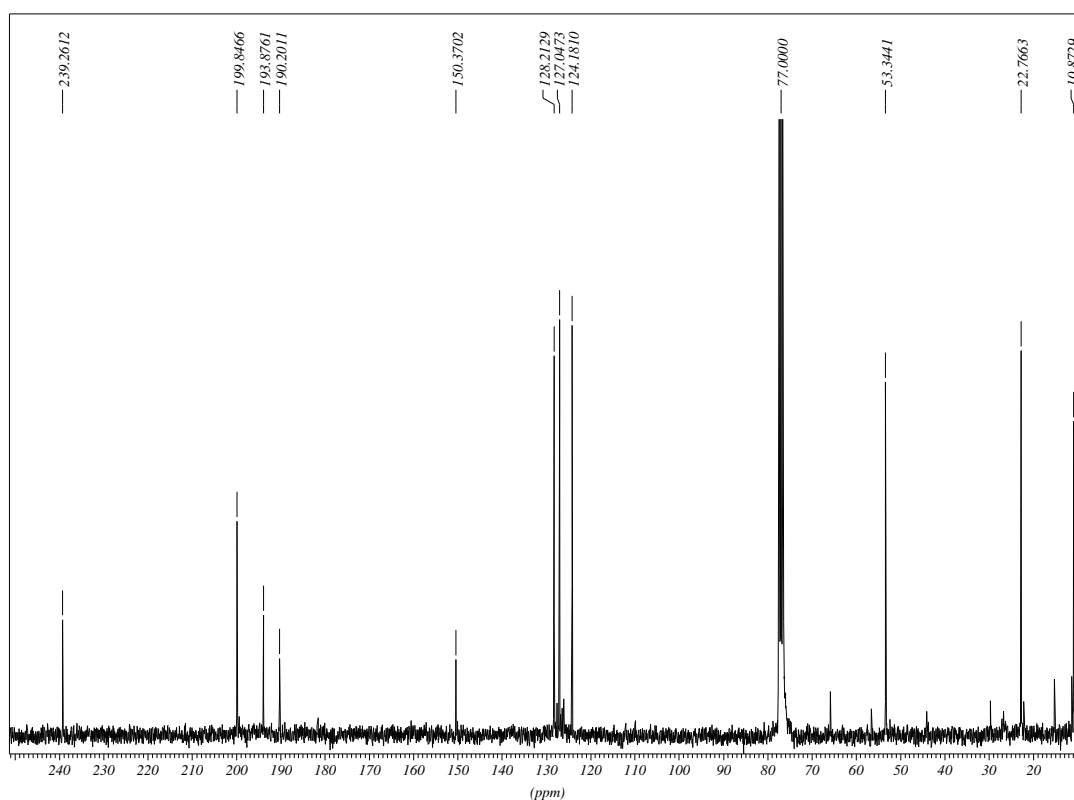


Figure 4.5 ^{13}C NMR spectrum of **14** in CDCl_3

A significant upfield shift of the chemical shift value of the C1 carbene carbon atom resonance of $\Delta\delta = 20 - 50$ ppm is observed in all recorded spectra (Table 4.2, 4.3), when compared to the ethoxycarbene analogues, although a smaller upfield shift for the arene carbon atoms are seen. This is ascribed to the greater ability of the nitrogen lone pair (compared to oxygen as heteroatom in these Fischer carbene complexes) to donate electron density to the electrophilic carbene carbon atom, stabilizing and shielding the nucleus.

On the other hand, a downfield shift of the terminal carbonyls is observed in the case of **8** and **9**, but for **10** - **14** the chemical shift values for the metal carbonyls are comparable with their ethoxy analogues characterized in Chapter 2, or previously reported in the case of the dirhenium compounds^[23]. A possible explanation could be found when looking at the X-ray structures of **8** and **9**: the configuration of these complexes changed from axial ethoxycarbenes to equatorial aminocarbene complexes. Complexes **10** - **15** retain the configuration shown originally in the ethoxy precursors, and their carbonyl groups are fairly insensitive to changes of substituents on ligands.

4.3.2 IR Spectroscopy

The infrared spectra of **8** - **15** were recorded in dichloromethane, instead of the usual hexane, due to the insolubility of these aminocarbene complexes in hexane. The theory of the ν_{CO} vibrations of bimetal nonacarbonyl compounds was discussed in Chapter 2. For the *eq*-[M₂(CO)₉L] complexes with C_s symmetry, a nine band pattern is expected in the IR spectrum, while five bands are expected for the *ax*-[M₂(CO)₉L] displaying C_{4v} symmetry. The five band pattern was observed for both **10** and **11**, the propylamine-substituted carbene complexes of dimanganese (Table 4.4). This indicated that the complexes retained their axial configuration during the nucleophilic substitution reaction.

Table 4.4 IR data in the carbonyl region of **10**, **11**^a

Complex	Carbonyl stretching frequencies (ν_{CO} , cm^{-1}) for pseudo- C_{4v} symmetry of $ax\text{-}[\text{Mn}_2(\text{CO})_9(\text{carbene})]$				
	A_1 (1)	A_1 (2)	E (1)	A_1 (3)	E (2)
10	2083 (w)	2029 (m)	1985 (vs)	1975 (s)	1926 (m)
11	2082 (m)	2012 (s)	1984 (vs)	1957 (s)	1928 (m)

a) DCM as solvent

In the case of **8**, **9**, **12** - **15**, the IR spectrum displayed only six bands, two of which are strong (Table 4.5). The observation of only six bands instead of the expected nine pattern for the C_s symmetry of an equatorially substituted $[\text{M}_2(\text{CO})_9\text{L}]$, can be explained by the following factors. In the first case, band overlap of the bands could have occurred due to solvent interaction. The assignments of the carbonyl stretching frequencies made in Table 4.5 are done as if this was the case. On the other hand, the solvent hexane is more inert towards the vibrational modes of the compounds and displays a greater resolution power in the spectra. In a non-polar hexane solution, the degeneracy of the band can be lifted, leading to the splitting of bands into two separate bands of different vibrational frequencies^[24]. Therefore, in the polar dichloromethane solvent fewer bands will be seen as when the spectrum is recorded in hexane. According to the rules specified by Nakamoto, if the A' and A'' vibrational modes become degenerate in dichloromethane, the resulting band can be assigned as an A'' mode. The same scenario was observed recently in our laboratories^[25], when the IR spectrum of a $[\text{M}(\text{CO})_5\text{L}]$ complex was recorded in dichloromethane. Recording the spectrum of the same compound in hexane led to the splitting of the E-band observed in dichloromethane into two separate bands as the degeneracy associated with the E-band was lifted.

Table 4.5 IR data in the carbonyl region of **8, 9, 12 - 15**^a

Complex	Carbonyl stretching frequencies (ν_{CO} , cm^{-1}) for C_s - symmetry of $eq\text{-}[M_2(\text{CO})_9(\text{carbene})]$					
	A'(1)	A'(2) and A'(3)	A''(1) and A'(4)	A''(2)	A'(5)	A'(6) and A''(3)
8	2084 (s)	2013 (s)	1987 (s)	1979 (s)	1960 (m)	1937 (m)
9	2082 (m)	2012 (s)	1984 (vs)	1977 (s)	1956 (m)	1935 (s)
12	2099 (w)	2035 (m)	1992 (vs)	1984 (s)	1961 (m)	1932 (s)
13	2098 (w)	2034 (m)	1990 (vs)	1983 (s)	1958 (m)	1931 (s)
14	2098 (w)	2034 (m)	1992 (vs)	1982 (s)	1959 (m)	1928 (m)
15	2098 (w)	2033 (m)	1990 (s)	1982 (s)	1958 (m)	1930 (s)

a) DCM as solvent

In the case of the dirhenium monocarbenes, all complexes show an equatorial configuration, but the amino-substituted dimanganese monocarbenes display equatorial configuration while the propylamine-substituted complexes are seen to be axially substituted.

Post and Watters reported the N-H vibrational frequencies obtained in the solid state^[21]. For their dimanganese and dirhenium aminomonocarbene complexes, two N-H stretch bands were observed in the region 3330 - 3405 cm^{-1} , assigned to a *cis* and *trans* configuration respectively, with the *cis* N-H stretch occurring at a higher wavenumber. Also observed were the N-H bend vibrational frequencies in the region 1530 - 1575 cm^{-1} . When inspecting the IR spectra recorded in solution for **8 - 15**, very weak N-H stretch bands were seen for **8, 9, 11** and **13** as listed in Table 4.6, but the N-H bands of the rest of the synthesized compounds were too weak to be observed in solution. No signal for the N-H bend was observed.

Table 4.6 N-H vibrational frequencies in the IR spectra of binuclear aminocarbene complexes^a

N-H stretch (cm ⁻¹)	8	9	11	13
<i>cis</i> N-H	3453	3473	3393	3479
<i>trans</i> N-H	3328	3348	3316	3351

a) DCM as solvent

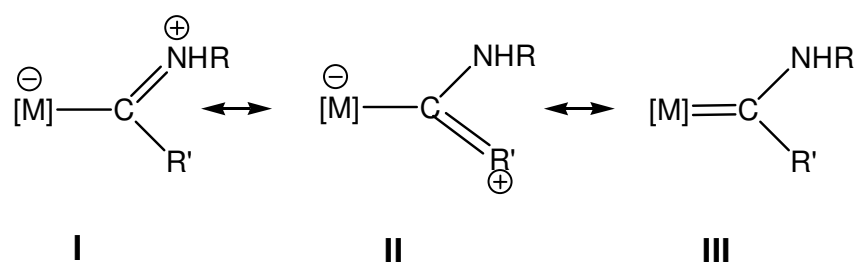


Figure 4.6 Limiting structures for carbene complexes

The structure of carbene complexes may be understood in terms of three limiting forms (I, II and III) that contribute to the stabilization of the formally electron-deficient carbene carbon (Figure 4.6). In limiting structure I the substituent R serves as a π -donor, while in limiting structure II substituent Y serves as a π -donor. Limiting structure III is stabilized by π -donation from the metal. Structural evidence^[26;27] led to the assumption that amine substituents are better π -donors than ethoxy substituents. Therefore the contribution of limiting structure I becomes more important where amine substituents are concerned, while metal π -donation is a larger contributing factor in the case of ethoxy substituents. Aryl substituents are generally poor π -donors to the carbene carbon and as a result carbene complexes with aryl substituents must either have substantial π -donation from the other substituent or a substantial contribution from limiting form III. Carbene complexes with π -

donor substituents (structures **I** and **II**) will have low M-C(carbene) bond orders and longer M-C(carbene) bond distances. The opposite is true for complexes with poor π -donor substituents (structure **III**).

Transition metal carbonyl bonds can be described as two resonance structures (Figure 4.7). In the case of the ethoxycarbene complex, metal π -donation is necessary to stabilize the electrophilic carbene carbon. Backbonding from the metal to the carbonyl carbon decreases, hence decreasing the M-C(carbonyl) bond order and simultaneously increasing the C(carbonyl)-O bond order. For aminocarbene complexes, less metal π -donation to the carbene carbon is necessary since the amine substituent stabilizes the carbene carbon. Backbonding from the metal to the carbonyl carbon increases resulting in a higher M-C(carbonyl) bond order and a decrease in the C(carbonyl)-O bond order. This explains the lower stretching frequencies observed on the spectra of complexes **10** and **11** compared to those of the ethoxycarbene complexes **2** and **3**, which is especially pronounced in the vibration wave number for the E(1) and E(2) bands.

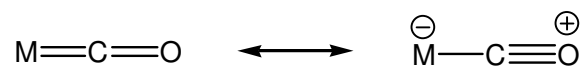


Figure 4.7 Resonance structures for M-C-O bonds

4.3.3 Mass Spectrometry

The mass spectral data of the aminocarbenes are summarized in Table 4.7 for the dirhenium compounds, and in Table 4.8 for the dimanganese complexes. In the case of **14** and **15**, no molecular ion peak was observed, and little information about the fragmentation pattern could be obtained. For the rest of the complexes, however, clear fragmentation patterns can be distinguished (Scheme 4.5, 4.6).

Table 4.7 Mass spectral data of the dirhenium aminocarbene complexes^a

Complex	m/z	Intensity (%)	Fragment ion
12	736	7	[M] ⁺
	409	52	[M – Re(CO) ₅] ⁺⁺
	381	13	[M – Re – 6CO] ⁺⁺
13	719	19	[M] ⁺
	664	7	[M – 2CO] ⁺
	636	6	[M – 3CO] ⁺
	393	94	[M – Re(CO) ₅] ⁺⁺
	365	24	[M – Re – 6CO] ⁺⁺
	337	6	[M – Re – 7CO] ⁺⁺

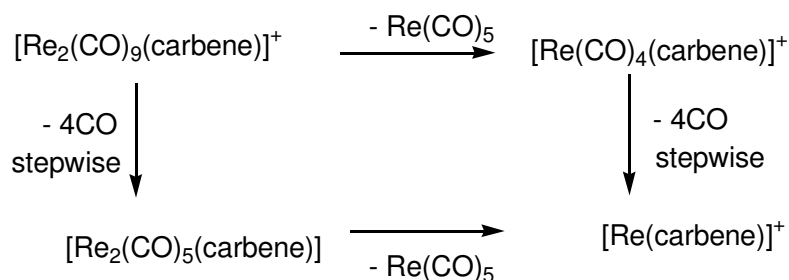
a) No [M⁺] was observed for **14** and **15**

The dirhenium aminocarbene complexes (**12**, **13**) lose the [Re(CO)₅]⁺-fragment by Re-Re bond cleavage first, followed by the loss of two further carbonyl ligands. This is the preferred fragmentation route, as seen by the intensities of the [M – Re(CO)₅]⁺⁺ fragment ion observed. The second route is the stepwise loss of carbonyl ligands after which the [Re(CO)₅]⁺-fragment is lost. The unusual fragmentation of the carbene ligand was not observed for the manganese analogues.

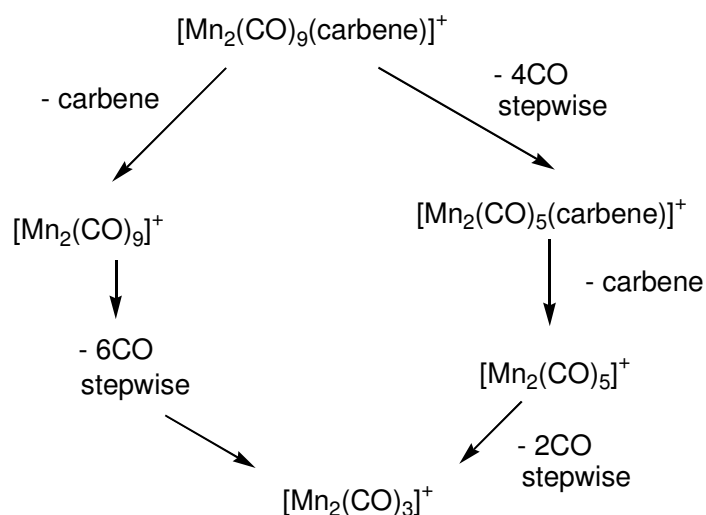
For the dimanganese aminocarbene complexes, no Mn-Mn bond breaking and loss of the Mn(CO)₅⁺-fragment ion can be seen. This can be ascribed to the much shorter Mn-Mn bondlength due to the smaller atomic radii of the manganese atoms when compared to rhenium. Instead, carbonyl ligands are lost first, followed by the carbene ligand. Subsequent loss of carbonyl ligands then continue until only a Mn₂(CO)₃-fragment remains. The other possible route is the fragmentation of the carbene ligand first, and then the stepwise fragmentation of carbonyl ligands. This early loss of the complete carbene ligand is an unusual feature in the mass spectrometry of carbene complexes.

Table 4.8 Mass spectral data of the dimanganese aminocarbene complexes

Complex	m/z	Intensity (%)	Fragment ion
8	473	4	$[M]^+$
	429	29	$[M - CO - NH_2]^+$
	362	12	$[M - (\text{carbene})]^+$
	278	44	$[M - 3CO - (\text{carbene})]^+$
	222	9	$[M - 5CO - (\text{carbene})]^+$
9	457	22	$[M]^+$
	401	14	$[M - 2CO]^+$
	345	10	$[M - 4CO]^+$
	306	15	$[M - 2CO - (\text{carbene})]^+$
	278	27	$[M - 3CO - (\text{carbene})]^+$
	250	37	$[M - 4CO - (\text{carbene})]^+$
	222	26	$[M - 5CO - (\text{carbene})]^+$
	194	26	$[M - 6CO - (\text{carbene})]^+$
10	515	-	$[M]^+$ n.o.
	459	38	$[M - 2CO]^+$
	306	19	$[M - 2CO - (\text{carbene})]^+$
11	499	12	$[M]^+$
	304	100	$[M - 2CO - (\text{carbene})]^+$
	278	32	$[M - 3CO - (\text{carbene})]^+$
	250	42	$[M - 4CO - (\text{carbene})]^+$
	222	29	$[M - 5CO - (\text{carbene})]^+$
	194	31	$[M - 6CO - (\text{carbene})]^+$



Scheme 4.5 Fragmentation routes for $[\text{Re}_2(\text{CO})_9(\text{carbene})]$



Scheme 4.6 Fragmentation pattern for $[\text{Mn}_2(\text{CO})_9(\text{carbene})]$

4.3.4 X-Ray Crystallography

Single crystal X-ray diffraction studies confirmed the molecular structure of complexes **8**, **9** and **11**. The X-ray structures corroborated the observations made from the infrared data: the dimanganese propylaminocarbene complexes have an axially substituted carbene ligand, while the dimanganese aminocarbene has an equatorial configuration. The complexes crystallized from a dichloromethane:hexane (1:1) solution by layering of the solvents,

yielding light orange crystals for **8**, **9** and **11** of good quality. Figures 4.8, 4.9 and 4.10 represent the ORTEP^[28] + POV-Ray^[29] plots of the geometry of these complexes. Once again, the same atom numbering system is used as employed in the previous chapters.

All three complexes crystallize in the monoclinic system, space group $P2_1/c$ with four molecules in the unit cell. Selected bond lengths and angles determined for the complexes are tabulated in Table 4.9 and 4.10 respectively, whilst the most important torsion angles are listed in Table 4.11. The complete crystallographic data of **8**, **9** and **11** are listed in Appendices 5, 6 and 7 respectively.

The average Mn-CO and Mn-Mn bond lengths of all three complexes are very similar to that of the ethoxycarbene precursors (Table 4.9). The Mn-C(carbene) bond length for **8** (2.019(3)Å), **9** (2.0275(16)Å) and **11** (1.994(5)Å) is significantly longer than the corresponding distance in **2** (1.933(7)Å) and **3** (1.932(2)Å), indicating a weaker Mn-C(carbene) bond due to less back bonding from the Mn metal centre to the carbene carbon. A very short C(carbene)-N bond length [**8** (1.315(4)Å); **9** (1.310(2)Å; **11** (1.351(12)Å)] indicates double bond character and implies a high degree of electron donation from the nitrogen lone pair to the electrophilic carbene carbon^[30]. This is also evident from the chemical shift of the carbene carbon atom at 269 ppm for **8**, 275 ppm for **9** and 255 ppm for **11** compared to 307 ppm for **2** and 301 ppm for **3**.

The Mn-C(carbene) bond is also slightly shorter for the axial carbene ligand in **11** compared to the equatorial carbene ligands of **8** and **9**. This means that the carbene carbon in the axial position must participate more in π -backbonding, due to the metal-metal bond *trans* to it, compared to when carbonyl ligands are *trans* to the carbene ligand in the equatorial position. As a result of this, the nitrogen atom in the axial carbene ligand shows less participation in the stabilization of the carbene carbon, as indicated by the slightly longer C(carbene)-N bond length of **11** than for **8** or **9**.

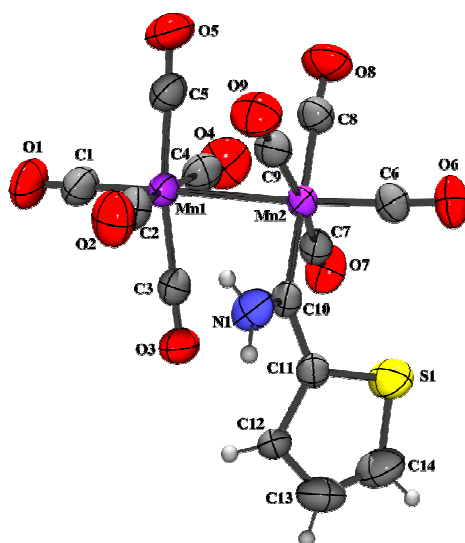


Figure 4.8 ORTEP + POV-Ray plot of the geometry of complex **8**

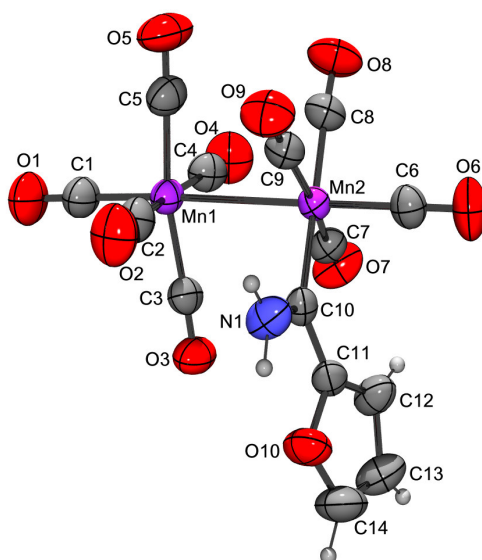


Figure 4.9 ORTEP + POV-Ray plot of the geometry of complex **9**

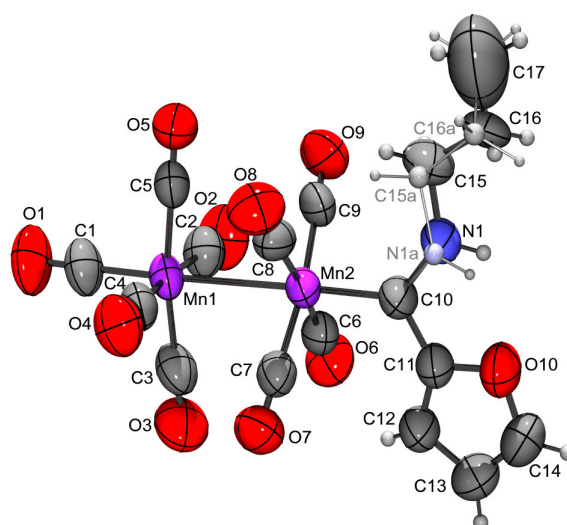


Figure 4.10 ORTEP + POV-Ray plot of the geometry of complex **11**

In contrast to the dimanganese ethoxycarbene **2** and the cleaved iodo-monomanganese carbene complex **7**, the thienyl ring of **8** is not close to being coplanar with the plane of the bonding geometry about the carbene carbon. The dihedral angle between the least-squares planes through (S(1), C(11), C(12), C(13) and C(14)) and through (C(10), C(11), N(1) and Mn(2)) is $39.7(1)^\circ$. The carbene ligand is in the preferred equatorial position, but to occupy this position, a deviation out of the plane is necessary to fit the thienyl S between the two closest carbonyl ligands C(6)-O(6) and C(7)-O(7). This deviation was also seen for the phenyl ring reported by Huttner and Regler for the *eq*-[Mn₂(CO)₉[C(OMe)Ph]] complex^[20]. The same is true for the furyl ring of complex **9**, but not **11**. The axial carbene ligand of the latter complex has enough space to adopt the preferred planar conformation.

From the X-ray crystal structure of **11**, a major and minor component was observed due to rotation of the propylamino-substituent around the N(1)-C(15) bond, such that the torsion angles of {C(9)-Mn(2)-C(10)-N(1) and C(8)-Mn(2)-C(10)-N(1)} for the two components are { $26.5(11)$ and $-64.8(11)^\circ$ } and { $67.2(11)$ and $-24.1(11)^\circ$ } respectively. The dihedral angles between the least-squares plane through (O(10), C(11), C(12), C(13) and C(14)), through (C(10), C(11), N(1), or Mn(2)) and (C(10), C(11), N(1a) and Mn(2)) are $12.9(5)^\circ$ and $9.5(6)^\circ$ respectively. This means that the furyl ring is close to

being coplanar with the plane of the bonding geometry about the carbene carbon, similar to the axial complexes **2** and **3**. The plane of the carbene carbon, furyl ring and nitrogen is approximately perpendicular to the equatorial plane of carbonyl ligands [C(10)-Mn(2)-CO (92 - 95 °)] and is in an intermediate position between the carbonyl ligands around Mn(2), as is evident from the torsion angles of $-47.3(5)^\circ$ and $42.5(5)^\circ$ for C(6)-Mn(2)-C(10)-C(11) and C(7)-Mn(2)-C(10)-C(11) respectively. As seen for the other axial binuclear carbene complexes (Chapter 2), the carbene ligand is in the *cis* configuration about the C(carbene)-N bond in **11**.

Table 4.9 Selected bond lengths of **8**, **9** and **11**

Atoms	Bond Lengths (Å)		
	8 (Y = S)	9 (Y = O)	11 (Y = O)
Mn(1)-C(1)	1.820(4)	1.8106(9)	1.798(5)
Mean Mn(1)-C(x) (x=2,3,4,5)	1.843(4)	1.847(2)	1.844(6)
Mn(1)-Mn(2)	2.9280(6)	2.9331(4)	2.9190(9)
Mean Mn(2)-C(x) (x=7,9) for 8,9 (x=6,7,8,9) for 11	1.845(3)	1.8435(18)	1.834(6)
Mn(2)-C(10)	2.019(3)	2.0275(16)	1.994(5)
C(10)-N(1)	1.315(4)	1.310(2)	1.351(12)
C(10)-C(11)	1.464(4)	1.452(2)	1.454(6)
C(11)-C(12)	1.496(4)	1.344(3)	1.329(7)
C(12)-C(13)	1.431(5)	1.414(3)	1.424(8)
C(13)-C(14)	1.321(7)	1.304(4)	1.312(9)
Mn(2)-C(6)	1.790(3)	1.7928(19)	-
Mn(2)-C(8)	1.836(3)	1.8355(19)	-
Y-C(11)	1.690(3)	1.376(2)	1.376(6)

Table 4.10 Selected bond angles of **8**, **9** and **11**

Atoms	Bond Angles (°)		
	8 (Y = S)	9 (Y = O)	11 (Y = O)
Mn(2)-C(10)-N(1)	125.7(2)	124.59(14)	124.1(7)
N(1)-C(10)-C(11)	109.8(3)	111.20(15)	111.9(6)
C(11)-C(10)-Mn(2)	124.4(2)	124.10(11)	122.2(3)
C(11)-Y-C(14)	93.09(19)	106.72(17)	107.0(5)
Y-C(11)-C(12)	111.5(2)	107.91(16)	108.2(4)
Y-C(14)-C(13)	113.2(3)	111.0(2)	110.3(6)
Y-C(11)-C(10)	122.8(2)	116.64(15)	118.0(4)
C(12)-C(13)-C(14)	116.8(4)	106.7(2)	106.4(6)
C(11)-C(12)-C(13)	105.4(3)	107.7(2)	108.0(5)

Complex **8** did not display major and minor components with the carbene ligand differing in orientation, unlike the disorder observed for **2** and **7**. This can be ascribed to the fact that the spatial similarity between the nearly coplanar ethoxy group and thienyl ring in the carbene ligand in both **2** and **7** is not present in the carbene ligand of **8**. The small NH₂-group of **8** and **9** can be accommodated adjacent to the carbonyl ligands C(2)-O(2), C(3)-O(3) and C(9)-O(9) in the equatorial plane. In **2** and **3**, with the carbene ligand adopting a *trans*-configuration about the C-O bond, the ethoxy group is too bulky to be accommodated and the carbene ligand is forced to occupy the axial position. This is also true in the case of **11**: the steric hindrance caused by the bulkier propylamine group forces the carbene ligand in the axial position, as it cannot be accommodated between the carbonyl ligands of the neighbouring metal centre. This is illustrated by the space-filling model of **9** in Figure 4.11 and **11** in Figure 4.12. Figure 4.11 shows the NH₂ group (N(1), H(1a), H(1b)) in relation to the adjacent carbonyl (C(9), O(9)) on Mn(2) and the adjacent carbonyl (C(2), O(2)) on Mn(1).

Table 4.11 Selected torsion angles of **8**, **9** and **11**

Atoms	Torsion Angles (°)	
	8 (Y = S)	9 (Y = O)
Mn(2)-C(10)-C(11)	- 142.7(2)	12.3(3)
Mn(2)-C(10)-C(11)-Y	38.8(3)	- 171.13(12)
C(9)-Mn(2)-C(10)-N(1)	10.4(3)	9.92(16)
C(7)-Mn(2)-C(10)-N(1)	- 160.4(3)	- 161.13(16)
Mn(1)-Mn(2)-C(10)-C(11)	106.7(2)	- 70.79(14)
C(8)-Mn(2)-Mn(1)-C(5)	- 40.16(16)	- 40.64(9)
C(9)-Mn(2)-Mn(1)-C(5)	49.18(15)	47.46(9)
Atoms	11 (Y = O)	
C(9)-Mn(2)-C(10)-N(1)	26.5(11)	
C(8)-Mn(2)-C(10)-N(1)	- 64.8(11)	
Mn(2)-C(10)-C(11)-C(12)	4.5(10)	
Mn(2)-C(10)-C(11)-Y	- 174.4(4)	
C(3)-Mn(1)-Mn(2)-C(6)	44.6(2)	
C(6)-Mn(2)-C(10)-C(11)	- 47.3(5)	
C(7)-Mn(2)-C(10)-C(11)	42.5(5)	

As can be seen from Figure 4.10, the nitrogen atom is orientated away from the adjacent carbonyl ligands. Steric hindrance is caused by the CH₂-group bonded to the nitrogen. Figure 4.12 illustrates the major component (C(15), H(15a), H(15b)) of the CH₂ of the disordered propylamine group in relation to the adjacent carbonyls (C(6),O(6) and C(7), O(7)) on Mn(2). The carbonyl (C(3), O(3)) is also shown space filled.

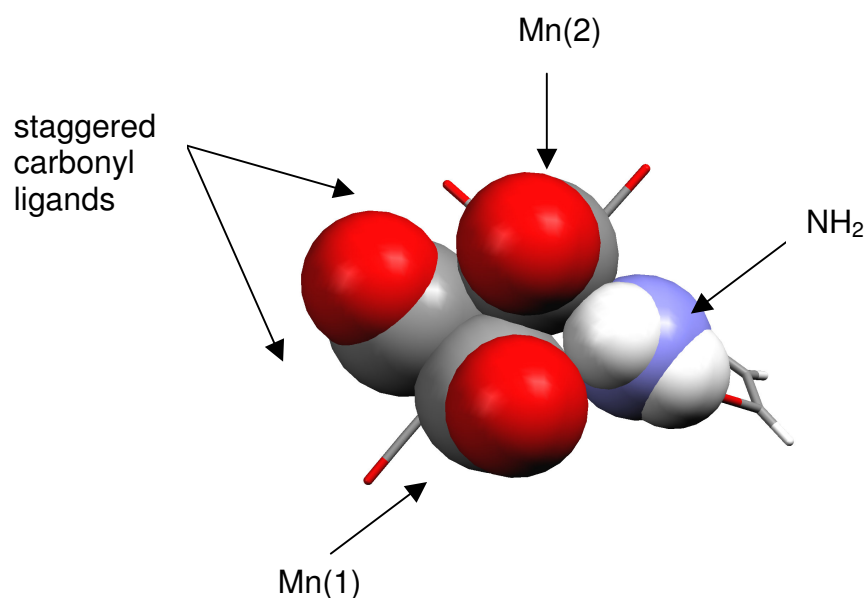


Figure 4.11 Space-filling model of **9** illustrating position of substituent NH₂-group on *eq*-carbene ligand

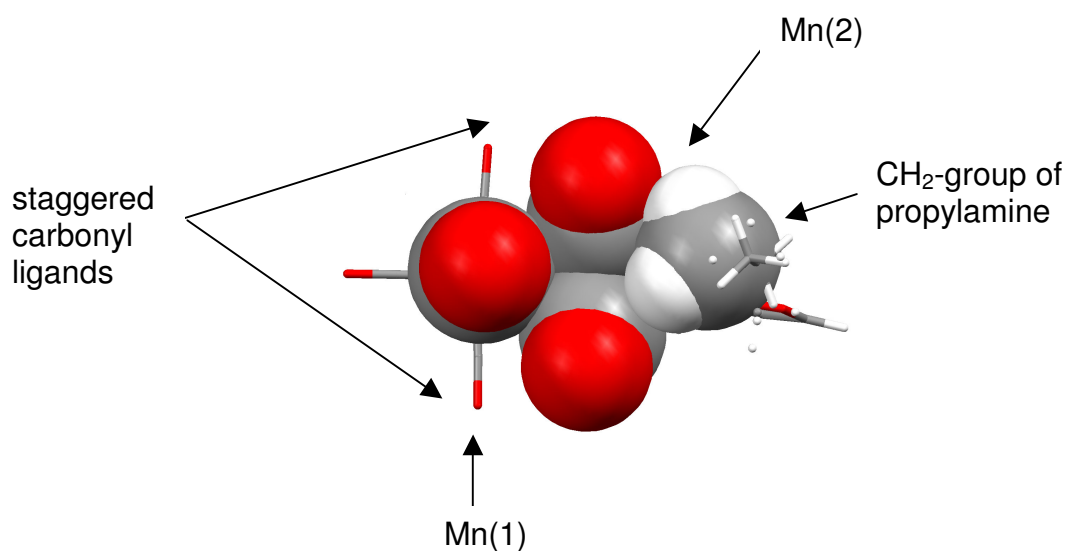


Figure 4.12 Space-filling model of **11** illustrating position of substituent propylamine on *ax*-carbene ligand

The torsion angles C(3)-Mn(1)-Mn(2)-C(6) for **11** is 44.6(2)°, similar to that of **2** and **3** (46.0(3)° and 45.97(10)°). For **8** and **9** the analogous C(8)-Mn(2)-

Mn(1)-C(5) torsion angles are $-40.16(16)^\circ$ and $-40.64(9)^\circ$ respectively. This indicates that the carbonyl ligands on adjacent manganese atoms are more staggered in **11**, the axially substituted binuclear carbene. **8** and **9** have a more eclipsed carbonyl conformation, but it is still significantly more staggered than the dirhenium monocarbene complex **5** (Chapter 2), with C(3)-Re(1)-Re(2)-C(8) $-30.93(19)^\circ$, due to the shorter Mn-Mn bond length.

When looking at the bonding geometry of the free thiophene and furan, and comparing it with the thienyl and furyl rings of **2**, **3**, **8**, **9** and **11**, it can be seen that the bond lengths of the aminocarbene complexes **8** and **9**, and especially **11**, more closely resemble that of the free heteroaryls (Table 2.8, 2.9 and 4.9). However, the bond angles of **2** and **3** are closer to the angles of the uncoordinated rings than **8**, **9** or **11** (Table 4.10). The high degree of electron donation from the nitrogen lone pair to the electrophilic carbene carbon means that there is less need for ring involvement in stabilizing the carbene carbon, so that the bonding lengths of the aminocarbene aryl rings are closer to that of the free rings. However, carbene ligands of these aminocarbene complexes are not coplanar with the plane of the bonding geometry about the carbene carbon, and the rings are twisted to fit in between the carbonyl ligands on the adjacent manganese atom. Presumably, that explains the unusually long C(11)-C(12) bond length ($1.496(4)\text{\AA}$) observed for **8**. This means that the bonding angles in these heteroaryl substituents will differ more significantly from the uncoordinated heteroaryls than the ethoxycarbene complexes.

4.4 Conclusions

Complexes **8** - **15** were synthesized and characterized spectroscopically, and final confirmation of the structures of these complexes in the solid state determined by X-ray diffraction. All the dirhenium aminocarbene complexes (**12** - **15**) were found to have the carbene ligand in an equatorial position, the Re-Re bond long enough to allow even bulky substituents on the carbene to be accommodated between the carbonyl ligands on the adjacent rhenium

atom. The dimanganese aminocarbenes (**8**, **9**) with an NH₂-group also have equatorial carbene ligands, but the bulky NH(C₃H₇)-substituted complexes (**10**, **11**) retain the axial configuration of their ethoxy precursors.

As proposed in Chapter 2, the position of the carbene ligand in [Mn₂(CO)₉(carbene)] complexes are determined by steric factors, due to the limitation of the short Mn-Mn bond. Bulky -OEt and -NH(C₃H₇) cannot be accommodated in an intermediate position between the adjacent carbonyl ligands, and therefore force the carbene ligand in an axial position.

The aminocarbene ligand is a weak π-acceptor with the electrophilic carbene carbon atom stabilized predominantly by electron donation from the nitrogen lone pair. The aminocarbene ligand would therefore preferentially occur at an equatorial position *trans* to a carbonyl ligand (a better π-acceptor ligand) in the electronically favourable position, unless forced by steric reasons into the axial position. On the other hand, the ethoxycarbene ligand is a better π-acceptor ligand in [Mn₂(CO)₉(carbene)] complexes, and can be better stabilized in an axial position. It is therefore possible to manipulate the position of the carbene ligand merely by varying the steric effects of the substituent on the carbene ligand. An attempt at aminolysis with an diethylamine and diisopropylamine did not prove successful, and it seems sterically not possible to accommodate a secondary amine substituent on the carbene ligand, even in the axial position.

4.5 References

1. A. Yamashita, *Tetrahedron Lett.* 27, **1986**, 5915.
2. C. Alvarez, A. Parlier, H. Rudler, R. Yefsah, J.C. Daran, C. Knobler, *Organometallics* 8, **1989**, 2253.
3. H. Rudler, A. Parlier, R. Yefsah, B. Denise, J.C. Daran, J. Vaissermann, C. Knobler, *J. Organomet. Chem.* 358, **1988**, 245.
4. C. Borel, L.S. Hegedus, S. Krebs, Y. Satoh, *J. Am. Chem. Soc.* 109, **1987**, 1101.
5. L.S. Hegedus, J.D.B. Miller, *J. Org. Chem.* 54, **1989**, 1249.
6. K.H. Dötz, H. Erben, K. Harms, *J. Chem. Soc., Chem. Commun.* **1989**, 692.
7. K.H. Dötz, T. Schaffer, K. Harms, *Angew. Chem. Int. Ed. Engl.* 29, **1990**, 176.
8. R. Aumann, P. Hinterding, *Chem. Ber.* 123, **1989**, 611.
9. W.D. Wulff, B.A. Anderson, L.D. Isaac, *Tetrahedron Lett.* 30, **1985**, 4061.
10. B.A. Anderson, W.D. Wulff, *J. Am. Chem. Soc.* 112, **1990**, 8615.
11. J.A. Connor, E.O. Fischer, *J. Chem. Soc. A* **1969**, 578.
12. U. Klabunde, E.O. Fischer, *J. Am. Chem. Soc.* 89, **1967**, 7141.
13. B. Crociani, *Reactions of Coordinated Ligands*, Plenum, New York **1986**, 553.
14. L. Canovese, F. Visente, P. Uguagliati, B. Crociani, *J. Organomet. Chem.* 535, **1997**, 69.
15. R. Imwinkelried, L.S. Hegedus, *Organometallics* 7, **1988**, 702.
16. F.R. Kreissl, W.J. Sieber, M. Wolfgruber, J. Riede, *Angew. Chem. Int. Ed. Engl.* 23, **1984**, 640.
17. F.R. Kreissl, W.J. Sieber, M. Wolfgrüber, *J. Organomet. Chem.* 270, **1984**, C45.
18. E.O. Fischer, E. Offhaus, *Chem. Ber.* 102, **1969**, 2449.

19. E.O. Fischer, E. Offhaus, J. Muller, D. Nöthe, *Chem. Ber.* 105, **1972**, 3027.
20. G. Huttner, D. Regler, *Chem. Ber.* 105, **1972**, 1230.
21. E.W. Post, K.L. Watters, *Inorg. Chim. Acta* 26, **1978**, 29.
22. H. Werner, E.O. Fischer, B. Heckl, C.G. Kreiter, *J. Organomet. Chem.* 28, **1971**, 367.
23. S. Lotz, M. Landman, D.I. Bezuidenhout, A.J. Olivier, D.C. Liles, P.H. van Rooyen, *J. Organomet. Chem.* 690, **2005**, 5929.
24. K. Nakamoto, *Infrared and Raman Spectra of Inorganic and Coordination Compounds. Part A: Theory and Applications in Inorganic Chemistry*, 5th ed. John Wiley & Sons, New York **1997**, 345.
25. E. van der Watt, *Synthesis of Fischer Carbene Complexes with Metal-containing Substituents*, University of Pretoria, **2006**.
26. M.Y. Darensbourg, D.J. Darensbourg, *Inorg. Chem.* 9, **1970**, 32.
27. J.A. Connor, J.P. Lloyd, *Chem. Rev.* **1970**, 3237.
28. L.J. Farrugia, *J. Appl. Crystallogr.* 30, **1997**, 565.
29. The POV-Ray Team, POV-Ray **2004**, URL: <http://www.pov-ray.org/download/>.
30. F.H. Allen, O. Kennard, D.G. Watson, L. Brammer, A.G. Orpen, R. Taylor, *J. Chem. Soc., Perkin Trans. II* **1987**, S1-S19.